View metadata, citation and similar papers at core.ac.uk
brought to you by CORE
provided by Elsevier - Publisher Connector

X-Ray Scattering and Electron Cryomicroscopy Study on the Effect of Carotenoid Biosynthesis to the Structure of *Chlorobium tepidum* Chlorosomes

T. P. Ikonen,* H. Li,† J. Pšenčík,‡ P. A. Laurinmäki,§ S. J. Butcher,§ N.-U. Frigaard,¶ R. E. Serimaa,* D. A. Bryant,† and R. Tuma§

*Department of Physical Sciences, University of Helsinki, Helsinki, Finland; †Department of Biochemistry and Molecular Biology, Pennsylvania State University, State College, Pennsylvania; ‡Department of Chemical Physics and Optics, Charles University, Prague, Czech Republic; §Institute of Biotechnology and Department of Biological and Environmental Sciences, University of Helsinki, Helsinki, Finland; and ¶Department of Molecular Biology, University of Copenhagen, Denmark

ABSTRACT Chlorosomes, the main antenna complexes of green photosynthetic bacteria, were isolated from null mutants of *Chlorobium tepidum*, each of which lacked one enzyme involved in the biosynthesis of carotenoids. The effects of the altered carotenoid composition on the structure of the chlorosomes were studied by means of x-ray scattering and electron cryomicroscopy. The chlorosomes from each mutant strain exhibited a lamellar arrangement of the bacteriochlorophyll *c* aggregates, which are the major constituents of the chlorosome interior. However, the carotenoid content and composition had a pronounced effect on chlorosome biogenesis and structure. The results indicate that carotenoids with a sufficiently long conjugated system are important for the biogenesis of the chlorosome baseplate. Defects in the baseplate structure affected the shape of the chlorosomes and were correlated with differences in the arrangement of lamellae and spacing between the lamellar planes of bacteriochlorophyll aggregates. In addition, comparisons among the various mutants enabled refinement of the assignments of the x-ray scattering peaks. While the main scattering peaks come from the lamellar structure of bacteriochlorophyll *c* aggregates, some minor peaks may originate from the paracrystalline arrangement of CsmA in the baseplate.

INTRODUCTION

Chlorosomes are the principal light-harvesting antenna structures of the photosynthetic machinery in green sulfur bacteria (*Chlorobiaceae*) and some filamentous anoxygenic phototrophs (*Chloroflexi*) (1,2). Among the photosynthetic antenna complexes found in nature, chlorosomes are unique because of their large size and because their main photosynthetic pigments (bacteriochlorophylls *c*, *d*, or *e*) are not bound to proteins but rather self-assemble into large aggregates. Typical chlorosomes have an ellipsoidal shape with a length of 100—200 nm, a width of 50–100 nm and a height of 10–30 nm (3). It is estimated that a single *Chlorobium* (*C.*) *tepidum* chlorosome contains more than 200,000 bacteriochlorophyll *c* (BChl *c*) molecules (4), which form the bulk of the chlorosome interior. Other major chlorosome constituents are carotenoids, which in total are present in ratios ranging from 5 to 25% (w/w) when compared to the main BChl component (5). Quinones (6), lipids, wax esters and proteins are also present. The mass ratio of BChl *c* to protein is ~2:1 (7); the protein and galactolipid constituents are localized on the surface of the chlorosome where they form an amphipathic, monolayer-like envelope (8,9) and contribute to the baseplate coupling the chlorosome to the plasma membrane and photosynthetic reaction centers.

While the external morphology of ellipsoidal chlorosomes is well established, their internal structure has been a subject of considerable debate. The first electron microscopy (EM) results contained evidence for striations with a width of 12–20 Å (10), but later work using freeze-fracture electron microscopy showed rod elements with a diameter of 5 nm in *C. aurantiacus* (11) and rod elements with a diameter of 10 nm in *C. limicola* (12). The first results with electron cryomicroscopy (cryo-EM) were presented in 2004 (13), and based upon additional cryo-EM (a tilt series, Fourier image analysis) and x-ray scattering, these methods again revealed 20 Å striations that were assigned to undulating lamellae. In cryo-EM, the samples are prepared in aqueous solutions and are imaged in vitreous water (14). In effect, this technique resolves the ambiguity caused by different staining and fixation procedures. Recent work comparing different fixation methods in electron imaging of chlorosomes has found evidence of lamellar striations in potassium permanganate fixed specimens of *C. tepidum* (15).

X-ray scattering from solutions of *C. tepidum* chlorosomes exhibits a prominent diffraction maximum at 21 Å, corresponding to the spacing of the striations observed in EM. In addition, three smaller maxima at higher angles are also discernible, and these provide evidence of paracrystalline order on the length scale of 10 Å. Based on these results, a lamellar model of BChl organization inside chlorosomes was proposed. In this model, the BChls are stacked on a

Submitted November 19, 2006, and accepted for publication March 13, 2007.

Address reprint requests to R. Tuma, Tel.: 35-89-1-915-9577; E-mail: roman.tuma@helsinki.fi.

H. Li's present address is Box 359690, Harborview Medical Center, 325 9th Ave., University of Washington, Seattle, WA 98104.

Editor: Jill Trewhella.

© 2007 by the Biophysical Society

0006-3495/07/07/620/09 $2.00

doi: 10.1529/biophysj.106.101444

disordered monoclinic lattice, where the *a*- and *b*-axes lie along the undulating chlorin ring stacks, or lamellae, and the *c*-axis is perpendicular to it. Carotenoids are proposed to be arranged between the farnesyl (the major esterifying alcohol of BChls in green sulfur bacteria) tails of the BChl, filling up the hydrophobic environment between the lamellae. An interaction between carotenoids and the farnesyl tails of the BChls was also found to be an essential part of BChl aggregation in the in vitro studies (16). This suggests that the hydrophobic effect may be the major driving force for pigment self-assembly in aqueous solutions, e.g., within bacterial cells.

The hot-spring dwelling, moderately thermophilic bacterium, *C. tepidum* (17), is currently the best characterized species among the chlorosome-containing bacteria. The sequencing of its genome (18), and the relative ease of genetic transfer (19,20) in this species make the generation of various knockout mutant strains possible. Among the gene products which have been successfully eliminated by mutation are chlorosome proteins (21), several enzymes involved in the biosynthesis of BChl *c* (22), and nearly all of the enzymes required for the synthesis of carotenoids (23,24), which led to mutants in which the chlorosomes are deficient in the targeted pigments (Fig. 1).

The chlorosomes produced by *C. tepidum* are resilient to drying and can even withstand elevated temperatures up to 120°C without major changes in the structural parameters observed in x-ray scattering (T. P. Ikonen and R. E. Serimaa, unpublished data). Recent results on brown-colored *Chlorobium* species show that while the lamellar structure is present in chlorosomes from *C. phaeovibrioides* and *C. phaeobacteroides*, both the morphology probed by cryo-EM and the molecular arrangement revealed by x-ray scattering show more disorder than is observed for *C. tepidum* chlorosomes (25). The ease of cultivation, manipulation, and the resilient, ordered chlorosomes produced by *C. tepidum*, makes this organism an ideal model system for studying the effects of pigment composition on chlorosome structure.

The effect of carotenoid deficiency on chlorosome development and structure was initially examined by Foidl and colleagues (26) by inhibiting the carotenoid biosynthesis in *C. aurantiacus* with 2-hydroxybiphenyl (HBP). The typical shape of the chlorosomes was not affected, although the chlorosomes were smaller, exhibited lower buoyant density, and lacked ~50% of the baseplate CsmA protein (26). The authors concluded that the colored carotenoids were largely dispensable for the phototropic growth of *C. aurantiacus*. They suggested in a parallel study that the carotenoids were located in the vicinity of the BChls in chlorosomes, and concluded that the organization of BChl *c* molecules is largely independent of the presence of the bulk of the carotenoids (27). In contrast, rather pronounced perturbations of optical spectra (5) and chlorosome morphology (28) were reported as a consequence of carotenoid inhibition by

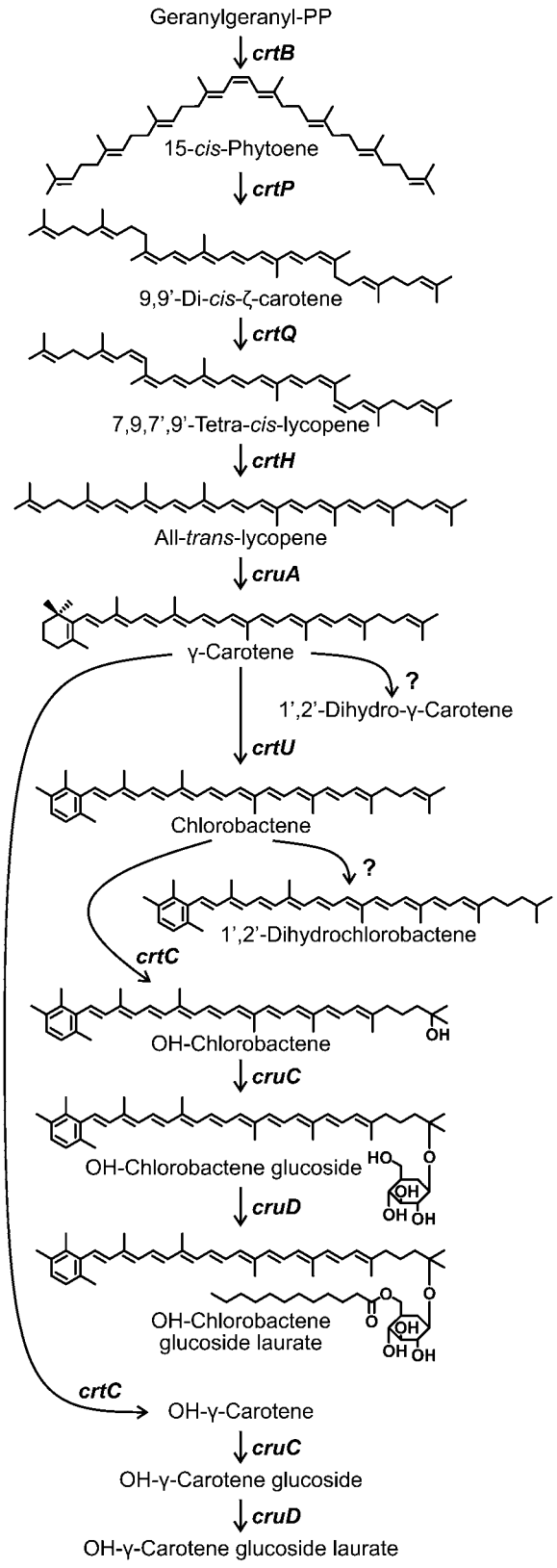

FIGURE 1 The proposed pathway of carotenoid biosynthesis in *C. tepidum* (based on (23) and (24)).

HBP in green sulfur bacteria. The rounded shape of the HBP-treated chlorosomes was explained by the lack of carotenoids, which are expected to be important for baseplate development (28). The HBP treatment also enabled the determination of ultrafast (<100 fs) energy transfer from carotenoids to bacteriochlorophylls in control chlorosomes of *C. phaeobacteroides* (29), confirming the close association between the two pigments.

In studies of complex, weakly ordered biological structures, one does not have the advantage (or problem) of large amounts of data, which in principle are contained in the hierarchical structures of living matter. On the contrary, the polymorphisms present in length scales above a few nanometers in most cases rapidly diminishes most of the information provided by a method that relies on the monodispersity of the objects under study, such as crystallography or cryo-EM reconstructions. While extraction of structural parameters from cryo-EM images of single particles may be limited by a low signal/noise ratio (e.g., features of size $<\sim 10$ Å are not resolved in single chlorosome images), the method provides an assessment of the variation in the chlorosome structure at intermediate resolutions (e.g., overall shape, organization of lamellae, presence of domains (25)). On the other hand, elastic scattering of x-rays from bulk samples provides reliable averages and can give structural parameters related to high-resolution features (e.g. lamellar spacing (13)). In any kind of measurement, detecting changes is easier than determining parameters or models in absolute terms. As noted above, *C. tepidum* provides many possibilities for changing the constituents of its chlorosomes and thus causing perturbations in their structure. In this article, we report the results from comparative structural studies on chlorosomes obtained from mutant strains, in which carotenoid biosynthesis of *C. tepidum* was disrupted by selectively disabling specific enzymes in the biosynthetic pathway.

MATERIALS AND METHODS

Sample preparation and characterization

The enzymes affecting the carotenoid biosynthesis in *C. tepidum* were eliminated by insertional inactivation as described previously (23). The six mutants employed in the present study each lacked one enzyme in the synthesis pathway (Fig. 1): phytoene synthase (CrtB), phytoene desaturase (CrtP), ζ-carotene desaturase (CrtQ), carotenoid *cis-trans* isomerase (CrtH), γ-carotene desaturase (CrtU), and carotenoid 1′,2′-hydratase (CrtC). The mutant strains were grown and chlorosomes were extracted as previously described (9,30). Cryo-EM images and optical absorption spectra from the sample solutions were collected using protocols described previously (13,25). Lamellar spacings were determined by Fourier method as described previously (13) and the mean values and standard deviations were obtained by averaging values from at least 20 chlorosomes of each type. Shape changes were assessed by counting the numbers of chlorosomes with the regular ellipsoidal shape (axial ratio at least 3:1) and those with irregular (round) appearance, respectively. Greater than 10 micrographs from two independent preparations were examined and a total of >500 chlorosomes were counted for each mutant as well as wild-type samples. The protein composition of the purified chlorosomes was analyzed by SDS-PAGE as described previously (9).

X-ray scattering

Samples having an $OD_{745\ nm}$ between 800 and 1100 were subjected to x-ray scattering analysis at beamline A2 in Hasylab (Hamburg, Germany). The x-ray wavelength was 1.5 Å, and the distance from the sample to the MAR CCD detector was 435 mm. The direct beam position on the detector was slightly offset from the center. This setup resulted in a large q-range of $q = 0.05$–0.84 1/Å. The length of the scattering vector q is defined as $q = 4 \times \pi \times \sin(\theta)/\lambda$, where θ is half of the scattering angle. The q-values were further calibrated with a sample of silver behenate.

The chlorosome solution samples were measured in a 90-μl volume cuvette with a silver frame and two 13-μm kapton windows. The buffer solution was measured after each sample. After transmission correction, this background was subtracted from sample scattering. Finally, the scattering patterns obtained from the two-dimensional detector were azimuthally averaged to obtain a one-dimensional curve. Some of the samples were also measured with the rotating anode SAXS/WAXS of an in-house instrument at the Department of Physical Sciences, University of Helsinki. Scattering profiles with the same q-range, but poorer signal/noise ratio were obtained from this apparatus.

RESULTS

Visible absorption and protein composition

The UV/VIS absorption spectra measured from the mutant chlorosome samples were similar to those of the wild-type with small differences being typical of batch-to-batch variation (Fig. 2 *A*). The 515 nm absorption band that corresponds to colored carotenoids is absent in the chlorosome samples from the *crtB*, *crtP*, and *crtQ* mutants. These results confirm the absence of carotenoids with more than seven conjugated double bonds in the chlorosomes of these mutants. The protein compositions of all mutant chlorosomes were similar to that of the wild-type (Fig. 2 *B*). In particular, the amounts of the essential baseplate protein CsmaA were equal to the wild-type level in all cases.

Electron microscopy

Cryo-EM was used to assess the overall shape and presence of domains in mutant chlorosomes and to compare the dimensions with those of the wild-type (Fig. 3). Wild-type chlorosomes were similar in appearance to those previously described (13).

crtB mutant

Half of the chlorosomes were round-irregular (nonellipsoidal) in shape ($\sim$100 nm diameter), while the other half exhibited the usual ellipsoidal shape with dimensions typical for wild-type chlorosomes ((150–200) $\times$ 50 nm). However, the typical pattern of parallel striations but with frequent discontinuities was observed in the ellipsoidal chlorosomes. The round-irregular chlorosomes appeared much denser,

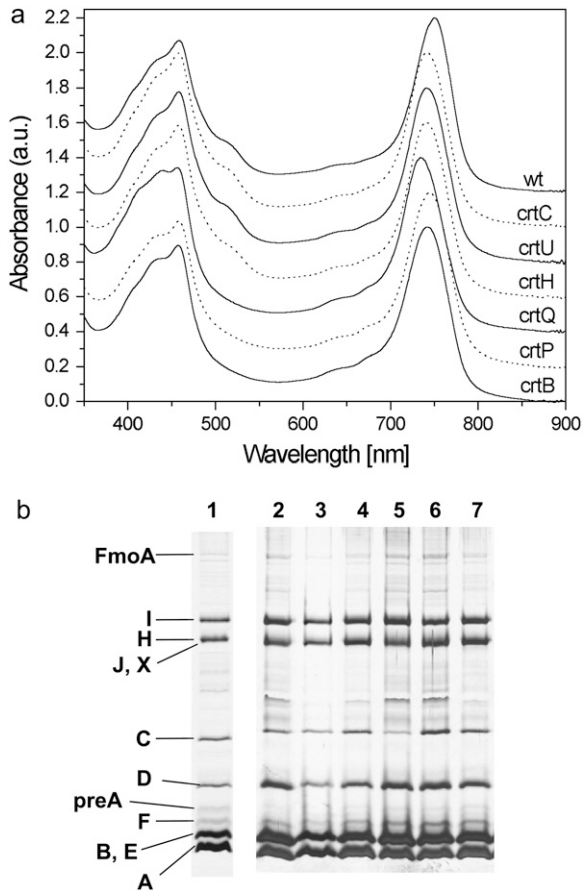

FIGURE 2 Spectral properties and protein compositions of wild-type and mutant chlorosomes. (*a*) Absorption spectra of chlorosomes from wild-type and species in which the carotenoid biosynthesis was disrupted at various steps. (*b*) SDS-PAGE of chlorosomes. Lane 1, wild-type; Lane 2, *crtB* mutant; Lane 3, *crtC* mutant; Lane 4, *crtH* mutant; Lane 5, *crtP* mutant; Lane 6, *crtQ* mutant; and Lane 7, *crtU* mutant. The identities of the various chlorosome proteins and FmoA, a minor contaminant, are indicated at the left.

indicating more spherical shape. These chlorosomes did not exhibit parallel striations, although lamellar domains were sometimes discernible. The lamellar spacing was determined for individual chlorosomes by computing power spectra from regions with pronounced striations. The lamellar spacing was 22 ± 2 Å (mean ± SD, obtained from analyses of many chlorosome images) for both the ellipsoidal and the round-irregular chlorosomes from the *crtB* mutant.

crtP mutant

The round-irregular shape persisted for ~30% of the chlorosomes. The overall dimensions of ellipsoidal chlorosomes in this sample were smaller ((100–150) × 40 nm) than those of the wild-type control.

crtQ mutant

Chlorosomes with the round-irregular shape were observed with frequency of ~20%. The chlorosomes exhibiting the normal ellipsoidal shape were smaller than wild-type chlorosomes.

crtH, crtU, crtC mutants

These mutants only formed ellipsoidal-shaped chlorosomes that exhibited lamellar striations, either parallel throughout the entire chlorosome or often with some discontinuities. However, these chlorosomes were again smaller ((100–150) × 40 nm) than those of the wild-type.

X-ray scattering

The x-ray scattering curves obtained for chlorosomes from the six carotenoid biosynthesis mutants are presented in Fig. 4. To extract numerical parameters, the experimental curves were fitted with two phenomenological models. The first model described the scattering in the *q*-region between 0.05 and 0.35 1/Å and consisted of a baseline defined by a power-law plus a constant, and three Gaussians corresponding to the three apparent peaks (see the *arrows* in Fig. 4). The second model was used for the wide-angle region (*q* from 0.45 to 0.80 1/Å). In this model, the baseline is represented by a broad Gaussian and a constant, and the three peaks observed in this region are fitted by Gaussians. The fitting employed the Levenberg-Marquardt optimization algorithm, which was implemented in the program Fityk (http://www.unipress.waw.pl/fityk/). The results from the fitting procedures are summarized in Table 1.

The scattering profiles of the mutant chlorosomes did not differ qualitatively from the wild-type control in the regions $q > 0.22$ 1/Å. A strong and broad diffraction maximum was observed between 0.26 and 0.29 1/Å, which corresponds to the 22–24 Å distance between the BChl *c* lamellae. The chlorosomes from bacteria in which the enzymes involved in the early synthesis of carotenoids were inactivated (*crtB*, *crtP*, *crtQ* mutant strains) reproducibly had the lamellar spacing ~1 Å larger than those of the wild-type (Table 1). For chlorosomes from the *crtB* mutant, this spacing was 23.3 Å, which is larger than the mean value determined from cryo-EM analysis of selected regions with pronounced striation. These tightly packed parts of lamellae typically exhibit a smaller spacing than the ensemble average value obtained by x-ray scattering, and the difference between the two values varies between different sample preparations (13,25). Chlorosomes containing only *cis*-phytoene from the *crtP* mutant had the largest observed spacing of 23.7 Å (Fig. 1).

The spacings observed for the other mutants were only slightly larger than those of the wild-type. It can be concluded that the lamellar spacing is basically the same as for wild-type chlorosomes in all chlorosomes that contain carotenoids with at least 11 conjugated double bonds, i.e., from tetra-*cis*-lycopene onward in the biosynthetic pathway.

Smaller maxima at 0.54, 0.67, and 0.76 1/Å, which were previously assigned to a tentative lattice structure of BChl

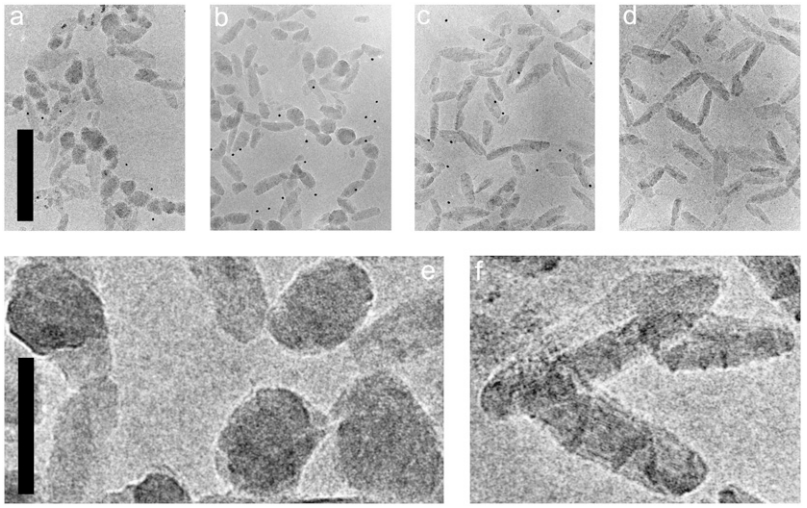

FIGURE 3 Comparison of overall shapes of chlorosomes obtained from mutant and wild-type strains of *C. tepidum*. Electron micrographs of samples embedded in vitreous ice: (*a*) *crtB* mutant, (*b*) *crtQ* mutant, (*c*) *crtH* mutant, and (*d*) wild-type chlorosomes. (*e*) A detailed view of round-irregular chlorosomes from *crtB* mutant, sometimes exhibiting domains of lamellar aggregates. (*f*) Ellipsoidal chlorosomes from *crtU* mutant with prevailing parallel striation. Scale bar is 400 nm for panels *a–d* and 100 nm for *e* and *f*.

within the lamellar planes, were present in the wide-angle region. Within the limits of the experimental precision, the positions and widths of these peaks did not change from one sample to another except for the highest angle 0.76 1/Å peak, which was found to be at slightly higher angles for chlorosomes from the *crtB*, *crtP*, and *crtQ* mutants than for the wild-type or the other mutant strains (see High-*q* peak in Table 1).

A feature at $q = 0.195$ 1/Å, which has not previously been assigned but which had been observed for all samples including those of brown-colored bacteria, occurred in the low angle region. This small peak was observed at the same position for chlorosomes from the *C. tepidum* carotenoid mutants as well as for the wild-type. The full width at half-maximum of this peak is 0.02 1/Å, a small value compared to the lamellar peak and the two first wide angle peaks, which have full width at half-maximum on the order of 0.11 1/Å. The position of this maximum varies very little from one sample to another. The standard deviation of the positions of this peak from all the samples studied was 0.002 1/Å, while the positions of the three high-*q* peaks had a mean ± SD of factor-of-2 larger, 0.004 1/Å, and the lamellar peak 0.009 1/Å. This lack of variability suggests that this peak may originate from a structure that is not directly related to the origin of the other peaks.

A clearly discernible broad maximum emerged at $q \sim 0.1$ 1/Å (Bragg spacing ~60 Å) in the scattering from chlorosomes of the *crtB* and *crtQ* mutants. Due to the large amount of scattering other than from this peak in the low-*q* region (described in the phenomenological model by a power-law decay), reliable fitting of this peak proved difficult. The most prominent peak is found in the *crtQ* mutant sample; a representative peak width of 0.1 1/Å was determined for this feature, which corresponds to an apparent coherent size of 60 Å.

DISCUSSION

Interpretation of x-ray scattering

In comparison with control chlorosomes, the scattering curves for chlorosomes from the *crtB* and *crtQ* mutants

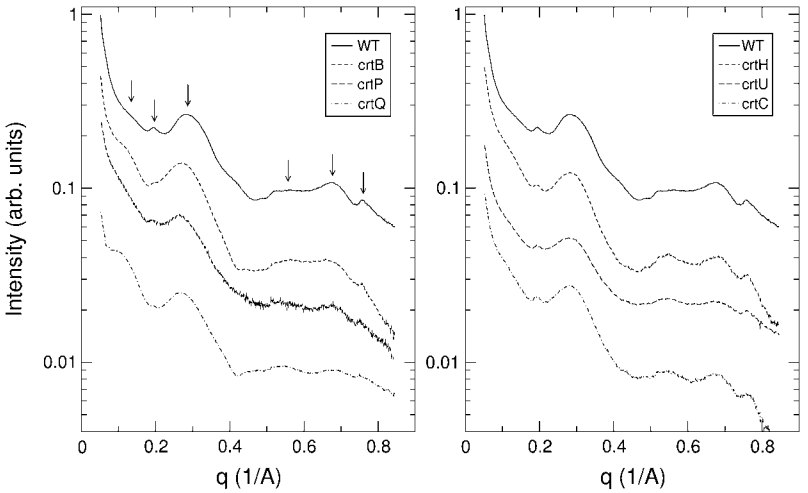

FIGURE 4 X-ray scattering from wild-type chlorosomes and chlorosomes with altered carotenoid composition. Left panel shows a comparison with wild-type and the samples in which the carotenoid composition was significantly altered due to mutations in the early portion of the biosynthetic pathway. The arrows mark the approximate positions of the peaks used in quantitative modeling. The right panel compares the results for wild-type chlorosomes with the samples from mutants in which the later stages of carotenoid biosynthesis are interrupted.

TABLE 1 Bragg spacings corresponding to some of the maxima observed in x-ray scattering

Strain	Lamellar peak* (0.265–0.285 1/Å) [Å]	High-q peak* (0.76 1/Å) [Å]	Sharp peak* (0.195 1/Å) [Å]	Percentage of round chlorosomes†
crtB	23.3	8.28	31.8	50
crtP	23.7	8.28	32.6	30
crtQ	23.4	8.28	31.9	20
crtH	22.2	8.24	32.4	0
crtU	22.2	8.24	32.4	0
crtC	22.4	8.20	32.4	0
Wild-type	22.0	8.21	31.8	0

*Relative errors of peak positions were <1% including batch-to-batch variation among the mutant samples and fitting errors.
†Percentages determined to within 5% standard error.

exhibited a clearly discernible feature at 0.1 1/Å (Bragg distance of 60 Å) that has not been assigned previously. Several possibilities were considered for the structural interpretation of this feature. Firstly, we considered the possibility that this feature reflects some internal structure of the chlorosome, in particular domains of lamellar aggregates as seen previously for the BChl *e* containing chlorosomes (25). If such a domain structure were to exist, it might be seen in x-ray scattering as the structure factor of the tightly packed domains, corresponding to an average domain-domain distance of 60 Å, or as the form factor of domains of roughly the same size. Different combinations of domain structures and form factors were calculated and compared to the experimental scattering pattern, but none was found to be completely satisfactory in explaining the broad peak observed in the data. Fig. 5 shows the low-angle scattering intensity from the chlorosome sample from the *crtQ* mutant, with the fit of the phenomenological power-law and the three-Gaussian model. As a first approximation, domains were represented by spheres with 55 Å radii and packed with regular spacing inside the chlorosome. Diffraction from this model exhibited a peak too narrow to reproduce the broad experimental feature (Fig. 5). Hence, a distribution of domain sizes (radii ranging from 40 to 60 Å) was introduced into the model, but this also failed to explain the broad peak. In this case, the position of the first form factor oscillation could be made to match the position of the 0.1 1/Å peak while the polydispersity in size distribution caused the oscillations in the form factors to cancel each other in the final structure factor (Fig. 5). In addition, structure factors were calculated from a distorted, tightly packed lattice of domains inside an ellipsoidal volume of the chlorosome. This refinement did not improve the fit (not shown). Although domains are also occasionally seen in *C. tepidum* chlorosomes, and were especially prominent in the round-irregular chlorosomes from the *crtB* and *crtP* mutants, the above modeling makes it unlikely that they contribute to x-ray scattering in this region. In addition, prominence of this scattering feature (most prominent in *crtQ*) does not correlate with the number of the domain-containing,

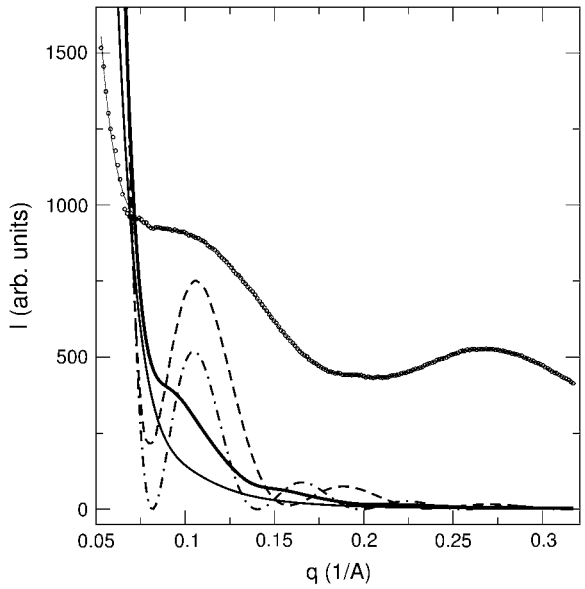

FIGURE 5 The low-angle portion of x-ray scattering intensity measured for chlorosomes from the *crtQ* mutant with the fit of the phenomenological model (*circles* and *thin solid line*) (32). The dashed line represents a model computed from a form factor of a single flat ellipsoidal cylinder with length 100 nm width, 50 nm, and height 8 nm. The thick solid line corresponds to scattering from a distribution of such ellipsoidal cylinders with a height distribution between 6 and 10 nm. The dot-dashed line is diffraction-computed for chlorosomes filled with spherical form factors of a 5.5 nm diameter. The thin solid line is diffraction from a distribution of spheres inside the chlorosome with 4.5–6.5 nm radii.

round-irregular chlorosomes (most frequently found for *crtB*).

Another possibility is that the 0.1 1/Å feature corresponds to the scattering from the outer shape of the chlorosome. Scattering intensity from an ellipsoidal cylinder 100-nm long, 50-nm wide, and 8-nm thick, corresponding to the shape of regular thin chlorosome is shown in Fig. 5. A thickness distribution between 6 and 10 nm leads to a scattering function (Fig. 5) that reproduces qualitatively the 0.1 1/Å feature. Due to the large size of the chlorosome, limited polydispersity in its overall form factor does not lead to complete cancellation of oscillations. This is in contrast to diffraction from smaller domains, as was described above.

A small peak at $q = 0.195$ 1/Å (Bragg spacing 32.2 Å) can be seen in all the samples studied, although its intensity varies from being prominent to nearly indistinguishable from the background. The stability in the position of this peak across all the samples, and its sharpness when compared to the other diffraction maxima, give a strong indication that this maximum does not originate from the same structure as the lamellar peaks. One possibility is the baseplate, which is considered to comprise a paracrystalline array of CsmA protein (11,31). Other evidence supporting this interpretation is derived from the correlation between the lower intensity of this peak (the peak is much weaker for the chlorosomes from the *crtB*, *crtP*, and *crtQ* mutants) and the appearance of the

rounded chlorosomes in the electron micrographs. The round chlorosomes, which lack the parallel striations, may also lack a properly assembled (paracrystalline) baseplate (28). Additionally, this peak was not observed for aggregates prepared in vitro from pure BChl *c* (M. Torkkeli, J. Pšenčík, A. Zupcanova, F. Vacha, R. Serimaa, and R. Tuma, unpublished results). Interestingly, another peak at 0.76 1/Å (Bragg spacing 8.2 Å) was missing from the scattering pattern obtained for pure BChl aggregates; this scattering peak may also emanate from the baseplate. Indeed, it is also extraordinarily sharp compared to the peaks assigned to the lamellar BChl *c* structures.

Correlations in x-ray data

In the lamellar model, the carotenoids are positioned between the planes of the chlorin stacks and are intermixed with the hydrophobic farnesyl tails of the BChl *c* molecules. The obvious perturbations of the lamellar spacing (23–24 Å Bragg spacing) found for chlorosomes of the *crtB*, *crtP*, and *crtQ* mutants in comparison with the wild-type (22 Å) clearly show that carotenoids have a pronounced effect on chlorosome assembly. Correlations between the positions of the major lamellar peak (22–24 Å) and those of other peaks may help to identify other structural features that are affected by carotenoids.

The only significant correlation (correlation coefficient 0.85) was found between the positions of the main lamellar peak and the 8.2 Å peak, respectively. Previously, the 8.2 Å peak was assigned to the reflection 110 from a putative monoclinic lamellar structure (13). As discussed above, this assignment is most likely incorrect because the peak is much sharper than the reflections 100, 010, and 001, and may be attributed to diffraction from the regular arrangement of CsmA proteins in the baseplate. In addition, no correlation was observed between the 001 and 010 or 100 peaks. The reflections 100 and 010 (0.67 and 0.54 1/Å peaks corresponding to 9.4 and 11.7 Å Bragg spacing, respectively) were observed at the same *q*-values as for previous *C. tepidum* samples (13), while the position of the 001 peak (~0.3 1/Å peak corresponding to ~20 Å Bragg spacing) is shifted. This implies that the distance between the planes may vary within the proposed lattice, although the arrangement of molecules within the plane remains unchanged.

It is interesting to note that the set of samples studied could be divided into two groups based on the position of the main ~22 Å peak: 1), wild-type-like (wild-type and the *crtH*, *crtU*, and *crtC* mutants), which have a mean lamellar peak Bragg distance of 22.2 Å, with standard deviation 0.2 Å; and 2), colored-carotenoid-deficient-like (the *crtB*, *crtP*, and *crtQ* mutant strains), with mean lamellar distance of 23.5 Å, mean ± SD 0.2 Å. Given this correlation, the same classification also applied to the 8.2 Å peak (wild-type-like spacing of 8.22 Å, mean ± SD 0.02 Å; colored-carotenoid-deficient-like mutants 8.28 Å, mean ± SD 0.004 Å).

Effect of the absence of specific carotenoids on chlorosome assembly

Although carotenoids are not absolutely essential for chlorosome assembly, they play an important role in chlorosome structure and function. In addition to their role in light harvesting and photoprotection, carotenoids were shown to induce BChl aggregate formation in the absence of lipids (16). Carotenoids reside in the hydrophobic space between the chlorin ring planes and thus are an integral part of the lamellar structure (25). It was found previously that partial inhibition of carotenoid synthesis affected chlorosome structure at the level of overall shape (round chlorosomes, (28)) as well as the lamellar spacing (slight increase, (25)). Similar effects were observed in the present work. In addition, the precise control over the accumulated intermediates in the present study provided an opportunity to correlate the carotenoid precursor structural and chemical properties with specific effects on assembly. The carotenoid synthesis pathway (Fig. 1) proceeds from geranylgeranyl diphosphate, a flexible and polar C_{20} chain, to conjugated molecules containing 40 carbons, such as lycopene and various other carotenoids. The spectroscopic changes observed for the mutant chlorosomes reflected the structure and spectral properties of the intermediates, which accumulated as a result of defects in the biosynthesis pathway (Fig. 2).

Disabling the first step in the pathway (*crtB* mutant, deficient in phytoene synthase) blocks the formation of all C_{40} carotenoids. The precursor, geranylgeranyl diphosphate, is a polar molecule and would not be incorporated within the hydrophobic interior of the chlorosome lamellae. The complete absence of carotenoids resulted in 50% of all chlorosomes being rounded in shape and lacking striations parallel to a unique direction. A similar phenotype was also observed for chlorosomes from *C. phaeobacteroides* in which carotenoid biosynthesis was inhibited by 2-hydroxybiphenyl (28). In this case, carotenoid deficiency correlated with decreased amounts of BChl *a*, which is exclusively associated with the baseplate. Similar correlations were observed for *crt* mutants of *C. tepidum*. All three mutants exhibiting round-irregular shape, contained 11 (*crtB*) to 13 mg (*crtP*, *crtQ*) of BChl *a* per 1 g of BChl *c* in their cells, which is a lower value compared to the wild-type (19 mg of BChl *a* per 1 g of BChl *c*) or the other mutants (16–18 mg of BChl *a* per 1 g of BChl *c* for *crtH*, *crtU*, and *crtC*) (23). In addition, the proximity of the baseplate was shown to correlate with the assembly of parallel lamellae (25), which are not observed in the round-irregular chlorosomes. Thus, carotenoid deficiency may cause overall morphological changes in chlorosomes via defects in baseplate assembly. This is further supported by the diminished intensity of the baseplate diffraction peaks (32 Å and 8.28 Å Bragg spacing) observed for these three mutants (Fig. 4).

The baseplate of a wild-type chlorosome is composed of many CsmA protein copies, each of which binds 1 BChl *a*

and no more than 1–2 carotenoid molecules per CsmA (21). From the wild-type amount of the baseplate (CsmA) protein in all *crt* mutants it is clear that even the rounded chlorosomes must contain CsmA, although its assembly into the baseplate might be compromised. We propose that carotenoids with at least 11 conjugated double bonds function as molecular glue and promote the assembly of CsmA proteins into the regular baseplate (26,28) and facilitate the incorporation of BChl *a*.

The average lamellar spacing observed by x-ray scattering increased from 22 to 23.3 Å in the absence of carotenoids. As the increase did not correlate with the number of round-irregular chlorosomes (Table 1) it is unlikely that the changes are caused merely by their presence. In addition, the spacing determined by cryo-EM was the same for round-irregular and ellipsoidal chlorosomes. Given the correlation between the lamellar and putative baseplate (8.2 Å) diffraction peaks, one may speculate that the structural changes in the baseplate may propagate into the larger spacing of the lamellae or vice versa.

The rounded chlorosomes did not possess any parallel striations, a situation similar to that of chlorosomes from brown bacteria (25). In contrast to the brown bacteria, sizable domains were discernible only occasionally. This suggests that while the baseplate is important for the development of the parallel striations, carotenoids may help to propagate order (parallel striations) within domains. Without the normal amount of carotenoids, BChl *c* aggregates form randomly and their order only rarely persists over sufficiently large distances to make the domains observable in cryo-EM.

Effect of carotenoid precursors on chlorosome structure

The introduction of long but nonconjugated phytoene molecules into the chlorosome structure (sample *crtP*) alleviated the baseplate defects somewhat and resulted in a larger proportion of chlorosomes with the normal ellipsoidal shape. It is known from studies of chlorosomes from brown-colored green sulfur bacteria (5,25) that phytoene accumulates inside chlorosomes and thus participates in the interactions between the BChl *c* farnesyl tails in a similar fashion to wild-type carotenoids. However, the bent 15-*cis*-phytoene molecules may not easily align with each other or with the farnesyl tails of BChl *c*. Thus, 15-*cis*-phytoene should occupy more space between the lamellae than the carotenoids normally present in wild-type chlorosomes and increase the lamellar spacing. Indeed, the largest lamellar spacing (x-ray scattering) was observed for the samples from the *crtP* mutant.

The addition of conjugated bonds to the chain by phytoene desaturase (the *crtQ* mutant sample) further decreased the extent of assembly defects (i.e., 20% of rounded chlorosomes were observed). However, the lamellar spacing is still larger than that of the wild-type. In addition, the broad feature in x-ray scattering at 0.1 1/Å is fairly pronounced, indicating that these chlorosomes may be thinner than the wild-type chlorosomes. This is presumably due to defects in propagating the lamellae further from the baseplate.

The decreased amount of BChl *a* and carotenoids may be partly responsible for the observed defects in the baseplate as stated above and previously suggested (23,26,28). However, it cannot explain differences in the percent occurrence of round-irregular chlorosomes in these three mutants. A plausible explanation can be given on the basis of differing carotenoid content: the *crtB* mutant contains no carotenoids at all and the *crtP* mutant contains only phytoene in a *cis* conformation, which might substitute less efficiently for the colored carotenoids in the baseplate and/or in the bacteriochlorophyll aggregates compared to di-*cis*-ζ-carotene in the *crtQ* mutant.

The addition of more conjugated bonds by ζ-carotene desaturase (the *crtH* mutant sample) forms tetra-*cis*-lycopene (and probably some all-*trans*-lycopene from photoisomerization), which already shows the wild-type optical properties with discernible absorption at 515 nm (Fig. 2), due to the presence of 11 conjugated bonds. The structural properties (except for the somewhat smaller size of chlorosomes) of this mutant are also very close to those of the wild-type chlorosomes, as far as can be determined from the cryo-EM and x-ray data. This suggests that the conjugated chain length and conformation are significant factors in attaining the native chlorosome structure. The wild-type-like shape of these chlorosomes can be taken as evidence for a wild-type baseplate. Since the *crtH* mutant can still form some γ-carotene and chlorobactene by photoisomerization (23), the assembly of CsmA monomers into the baseplate presumably proceeds in a relatively normal manner.

The other enzymes that were eliminated genetically in this study do not seem to play a major role in the self-assembly of the internal structure of the chlorosome. These other enzymes are in the pathway downstream of the carotenoid *cis-trans* isomerase and synthesize carotenoids that are chemically distinct from lycopene but that nevertheless contain a long, conjugated chain. These chemical differences may be useful in photoprotection, light-harvesting, and excitation energy transfer within the BChl-carotenoid aggregate, but they do not greatly affect the nanoscale structure of the BChl *c* aggregates nor do they significantly perturb the light harvesting capabilities or growth rates of these mutants. This indicates that lycopene and related compounds function well once the threshold value for number of conjugated double bonds is met.

Technical assistance of Ulla Vainio from Dept. of Physical Sciences, University of Helsinki, and Dr. Sergio Funari from Hasylab beamline A2 is gratefully acknowledged. We thank the Electron Microscopy Unit, Institute of Biotechnology, University of Helsinki for the cryo-EM facilities.

This research was funded by grant No. DE-FG02-94ER20137 from the U.S. Department of Energy to D.A.B., Academy of Finland (grant No. 1208661 to S.J.B., grant No. 211986 to R.T., and grant No. 112790 to

R.E.S.); University of Helsinki nanofunding (S.J.B.); Biocentrum Helsinki (S.J.B.); and Czech Science Foundation and Czech Ministry of Education, Youth and Sports (contracts No. 206/05/2739 and No. MSM0021620835 to J.P.).

REFERENCES

1. Blankenship, R. E., J. M. Olson, and M. Miller. 1995. Antenna complexes from green photosynthetic bacteria. *In* Anoxygenic Photosynthetic Bacteria. R. E. Blankenship, M. T. Madigan, and C. E. Bauer, editors. Kluwer Academic Publisher, Dordrecht, The Netherlands.
2. Frigaard, N. U., and D. A. Bryant. 2006. Chlorosomes: antenna organelles in photosynthetic green bacteria. *In* Microbiology Monographs, Vol. 2. Complex Intracellular Structures in Prokaryotes. J. M. Shively, editor. Springer, Berlin. 79–114.
3. Martinez-Planells, A., J. B. Arellano, C. A. Borrego, C. Lopez-Iglesias, F. Gich, and J. S. Garcia-Gil. 2002. Determination of the topography and biometry of chlorosomes by atomic force microscopy. *Photosynth. Res.* 71:83–90.
4. Montano, G. A., B. P. Bowen, J. T. LaBelle, N. W. Woodbury, V. B. Pizziconi, and R. E. Blankenship. 2003. Characterization of *Chlorobium tepidum* chlorosomes: a calculation of bacteriochlorophyll *c* per chlorosome and oligomer modeling. *Biophys. J.* 85:2560–2565.
5. Arellano, J. B., J. Pšenčík, C. M. Borrego, Y. Z. Ma, R. Guyoneaud, J. Garcia-Gil, and T. Gillbro. 2000. Effect of carotenoid biosynthesis inhibition on the chlorosome organization in *Chlorobium phaeobacteroides* strain CL1401. *Photochem. Photobiol.* 71:715–723.
6. Frigaard, N. U., S. Takaichi, M. Hirota, K. Shimada, and K. Matsuura. 1997. Quinones in chlorosomes of green sulfur bacteria and their role in the redox-dependent fluorescence studied in chlorosome-like bacteriochlorophyll *c* aggregates. *Arch. Microbiol.* 167:343–349.
7. Chung, S., G. Frank, H. Zuber, and D. A. Bryant. 1994. Genes encoding 2 chlorosome components from the green sulfur bacteria *Chlorobium vibrioforme* strain 8327d and *Chlorobium tepidum*. *Photosynth. Res.* 41:261–275.
8. Olson, J. M. 1998. Chlorophyll organization and function in green photosynthetic bacteria. *Photochem. Photobiol.* 67:61–75.
9. Li, H., N. U. Frigaard, and D. A. Bryant. 2006. Molecular contacts for chlorosome envelope proteins revealed by cross-linking studies with chlorosomes from *Chlorobium tepidum*. *Biochemistry.* 45:9095–9103.
10. Cohen-Bazire, G., N. Pfennig, and R. Kunisawa. 1964. The fine structure of green bacteria. *J. Cell Biol.* 22:207–225.
11. Staehelin, L. A., J. R. Golecki, R. C. Fuller, and G. Drews. 1978. Visualization of the supramolecular architecture of chlorosome (*Chlorobium* type vesicles) in freeze-fractured cells of *Chloroflexus aurantiacus*. *Arch. Microbiol.* 119:269–277.
12. Staehelin, L. A., J. R. Golecki, and G. Drews. 1980. Supramolecular organization of chlorosome (*Chlorobium* vesicles) and of their membrane attachment site in *Chlorobium limicola*. *Biochim. Biophys. Acta.* 589:30–45.
13. Pšenčík, J., T. P. Ikonen, P. Laurinmäki, M. C. Merckel, S. J. Butcher, R. E. Serimaa, and R. Tuma. 2004. Lamellar organization of pigments in chlorosomes, the light harvesting complexes of green photosynthetic bacteria. *Biophys. J.* 87:1165–1172.
14. Dubochet, J., M. Adrian, J. J. Chang, J. C. Homo, J. Lepault, A. W. McDowall, and P. Schultz. 1988. Cryo-electron microscopy of vitrified specimens. *Q. Rev. Biophys.* 21:129–228.
15. Hohmann-Marriott, M. F., R. E. Blankenship, and R. W. Roberson. 2005. The ultrastructure of *Chlorobium tepidum* chlorosomes revealed by electron microscopy. *Photosynth. Res.* 86:145–154.
16. Klinger, P., J. B. Arellano, F. E. Vacha, J. Hala, and J. Pšenčík. 2004. Effect of carotenoids and monogalactosyl diglyceride on bacteriochlorophyll *c* aggregates in aqueous buffer: implications for the self-assembly of chlorosomes. *Photochem. Photobiol.* 80:572–578.
17. Wahlund, T. M., C. R. Woese, R. W. Castenholz, and M. T. Madigan. 1991. A thermophilic green sulfur bacterium from New Zealand hot-springs, *Chlorobium tepidum* sp. *nov. Arch. Microbiol.* 156: 81–90.
18. Eisen, J. A., K. E. Nelson, I. T. Paulsen, J. F. Heidelberg, M. Wu, R. J. Dodson, R. Deboy, M. L. Gwinn, W. C. Nelson, D. H. Haft, E. K. Hickey, J. D. Peterson, A. S. Durkin, J. L. Kolonay, F. Yang, I. Holt, L. A. Umayam, T. Mason, M. Brenner, T. P. Shea, D. Parksey, W. C. Nierman, T. V. Feldblyum, C. L. Hansen, M. B. Craven, D. Radune, J. Vamathevan, H. Khouri, O. White, T. M. Gruber, K. A. Ketchum, J. C. Venter, H. Tettelin, D. A. Bryant, and C. M. Fraser. 2002. The complete genome sequence of *Chlorobium tepidum* TLS, a photosynthetic, anaerobic, green-sulfur bacterium. *Proc. Natl. Acad. Sci. USA.* 99:9509–9514.
19. Wahlund, T. M., and M. T. Madigan. 1995. Genetic transfer by conjugation in the thermophilic green sulfur bacterium *Chlorobium tepidum*. *J. Bacteriol.* 177:2583–2588.
20. Frigaard, N. U., G. D. Voigt, and D. A. Bryant. 2002. *Chlorobium tepidum* mutant lacking bacteriochlorophyll *c* made by inactivation of the *bchK* gene, encoding bacteriochlorophyll *c* synthase. *J. Bacteriol.* 184:3368–3376.
21. Frigaard, N. U., H. Li, K. J. Milks, and D. A. Bryant. 2004. Nine mutants of *Chlorobium tepidum* each unable to synthesize a different chlorosome protein still assemble functional chlorosomes. *J. Bacteriol.* 186:646–653.
22. Frigaard, N. U., H. Li, P. Martinsson, S. K. Das, H. A. Frank, T. J. Aartsma, and D. A. Bryant. 2005. Isolation and characterization of carotenosomes from a bacteriochlorophyll *c*-less mutant of *Chlorobium tepidum*. *Photosynth. Res.* 86:101–111.
23. Frigaard, N. U., J. A. Maresca, C. E. Yunker, A. D. Jones, and D. A. Bryant. 2004. Genetic manipulation of carotenoid biosynthesis in the green sulfur bacterium *Chlorobium tepidum*. *J. Bacteriol.* 186:5210–5220.
24. Maresca, J. A., and D. A. Bryant. 2006. Two genes encoding new carotenoid-modifying enzymes in the green sulfur bacterium *Chlorobium tepidum*. *J. Bacteriol.* 188:6217–6223.
25. Pšenčík, J., J. B. Arellano, T. P. Ikonen, C. M. Borrego, P. A. Laurinmaki, S. J. Butcher, R. E. Serimaa, and R. Tuma. 2006. Internal structure of chlorosomes from brown-colored *Chlorobium* species and the role of carotenoids in their assembly. *Biophys. J.* 91: 1433–1440.
26. Foidl, M., J. R. Golecki, and J. Oelze. 1997. Phototrophic growth and chlorosome formation in *Chloroflexus aurantiacus* under conditions of carotenoid deficiency. *Photosynth. Res.* 54:219–226.
27. Frese, R., U. Oberheide, I. H. M. van Stokkum, R. van Grondelle, M. Foidl, J. Oelze, and H. van Amerongen. 1997. The organization of bacteriochlorophyll *c* in chlorosomes from *Chloroflexus aurantiacus* and the structural role of carotenoids and protein—an absorption, linear dichroism, circular dichroism and Stark spectroscopy study. *Photosynth. Res.* 54:115–126.
28. Arellano, J. B., C. M. Borrego, A. Martinez-Planells, and L. J. Garcia-Gil. 2001. Effect of carotenoid deficiency on cells and chlorosomes of *Chlorobium phaeobacteroides*. *Arch. Microbiol.* 175:226–233.
29. Pšenčík, J., Y. Z. Ma, J. B. Arellano, J. Garcia-Gil, A. R. Holzwarth, and T. Gillbro. 2002. Excitation energy transfer in chlorosomes of *Chlorobium phaeobacteroides* strain CL1401: the role of carotenoids. *Photosynth. Res.* 71:5–18.
30. Vassilieva, E. V., V. L. Stirewalt, C. U. Jakobs, N. U. Frigaard, K. Inoue-Sakamoto, M. A. Baker, A. Sotak, and D. A. Bryant. 2002. Subcellular localization of chlorosome proteins in *Chlorobium tepidum* and characterization of three new chlorosome proteins: CsmF, CsrnH, and CsmX. *Biochemistry.* 41:4358–4370.
31. Bryant, D. A., E. V. Vassilieva, N. U. Frigaard, and H. Li. 2002. Selective protein extraction from *Chlorobium tepidum* chlorosomes using detergents. Evidence that CsmA forms multimers and binds bacteriochlorophyll *a*. *Biochemistry.* 41:14403–14411.
32. Pedersen, J. S. 1997. Analysis of small-angle scattering data from colloids and polymer solutions: modeling and least-squares fitting. *Adv. Colloid Interface Sci.* 70:171–210.